FROM FS – NS: INFLUENCE OF THE PULSE DURATION ONTO THE MATERIAL REMOVAL RATE AND MACHINING QUALITY FOR METALS

Paper IM309

Benjamin Lauer[1], Beat Neuenschwander [1], Beat Jaeggi[1], Marc Schmid[1]

[1] Bern University of Applied Science, Institute of Applied Laser, Photonics and Surface Technologies, Pestalozzistrasse 20, 3400 Burgdorf, Switzerland

Abstract

When high requirements concerning machining quality are demanded, ultra short laser pulses from a few 100fs to 10ps may be the tool of choice. For these pulses it is known that the removal rate and machining quality slightly increases with shorter pulse duration. But as cost-effectiveness is also a key factor for a successful transfer of a technology to industrial applications, these systems compete against more cost effective systems with pulse durations from several 10ps to a few ns. It was found in previous work that the removal rate for metals strongly decreases if the pulse duration is raised from 10ps to 50ps. In contrast to this dramatic drop new experiments show that the impact is much weaker for a further increase to several 100 ps and that the removal rate even increases when the pulse duration is further raised into the ns-regime. A systematic study of the removal rate and the machining quality for this longer pulse durations will be presented and the results will be pulled together with the previous ones for pulse durations of several 100fs to 50ps. Further it will be shown how operating factors from the laser system itself may influence its own applicability.

Introduction

Systems with 10 ps or shorter pulses show clear advantages concerning machining quality, heat affected zone, debris etc. [1-4]. But even if the excellent machining quality is one of the key advantages of these systems, it may be more cost effective to use fiber based amplifier technologies without CPA. The pulse duration of these systems is in the range of several 10 ps, [5-7]. For metals the ablation efficiency significantly drops by about a factor of 5 when the pulse duration is raised from 10 ps to 50 ps [8, 9], for non metals this drop is less pronounced but still present as shown by the authors at Icaleo 2011[10].

Another alternative may be offered by actively Q-switched DPSS with pulse durations in the sub-ns range. But the results of these systems should also be compared with fiber based Q-Switched systems with pulse durations in the short ns-range.

The characteristics of the measured ablation efficiency as a function of the pulse duration implies, that the efficiency could increase when the pulse duration is reduced from 10 ps into the sub ps regime. Results corroborating this belief have been reported in [11-13]. This all encourages the development of fiber based ultra short pulsed systems in the fs-regime which can be driven to high average powers by succeeding amplifier stages; recently more than 1 kW average power with fs – laser pulses were demonstrated [14,15]. From this point of view sub – ps systems could to be very attractive for laser micro processing.

Therefore investigations concerning the removal rate and the machining quality have been done for the pulse durations of 10 ps, 50 ps, 520 ps and 4 ns at 1064 nm wavelength on cu-DHP and stainless steel 1.4301 and 1.3343. 1.3343 was investigated in initial state (max. 262HB, ca. 27HRC) and hardened (64HRC). Investigations in fs-regime will be done later.

Theory

Ablation

For ultra short pulses the heat-transfer process in metals is described with the two temperature model [1, 16-20] where the temperatures of the electrons and the lattice are treated separately. The results of the model and the experiments show, that the ablation depth z_{abl} can be written in a first approximation as a function of the fluence ϕ (average fluence is used):

$$z_{abl} = \delta \cdot \ln\left(\frac{\phi}{\phi_{th}}\right) \tag{1}$$

$$\phi = \frac{E_p}{\pi \cdot w_0^2} \tag{2}$$

with ϕ_{th} the threshold fluence, δ the energy penetration depth, E_p the pulsenergy and w_0 the radius of the laser focus. Frequently two different ablation regimes are reported [18, 21]: firstly the low fluence regime where the optical penetration depth dominates and secondly the high fluence regime where the energy transport is dominated by the heat diffusion of the hot electrons. In [22] it is shown, that for a top hat beam the efficiency of the ablation process depends on the ratio between the threshold fluence and the applied fluence ϕ_{th}/ϕ. The efficiency shows a maximum value of 1/e, i.e. about 37%. At this point of maximum efficiency the ablated volume per pulse reads:

$$\Delta V_{Pulse} = \pi \cdot w_0^2 \cdot \delta \tag{3}$$

From this one can calculate the maximum removal rate per average power which reads for a top hat beam:

$$\frac{\dot{V}_{max}}{P_{av}} = \eta_{max} \cdot \frac{\delta}{\phi_{th}} = \frac{1}{e} \cdot \frac{\delta}{\phi_{th}} \tag{4}$$

The removal rate finally depends on the energy penetration depth δ and the threshold fluence ϕ_{th}.

Similar calculations have been done for a Gaussian shaped beam as emitted by most ultra short pulsed systems [22, 24]. Again a maximum removal rate per average power (ablation efficiency) is observed:

$$\frac{\dot{V}_{max}}{P_{av}} = \frac{2}{e^2} \cdot \frac{\delta}{\phi_{th}} \tag{5}$$

The ablated volume per pulse at this optimum point is again given by (3) i.e. this maximum efficiency is again obtained at a corresponding fluence. It has to be pointed out that the maximum value of the removal rate (5) is only obtained at this optimum point. A general expression for the removal rate of a Gaussian beam is also developed in [23, 24] and reads:

$$\dot{V} = \frac{1}{4} \cdot \pi \cdot w_0^2 \cdot \delta \cdot f \cdot \ln^2\left(2\frac{\phi}{\phi_{th}}\right) \tag{6}$$

Without depending on frequency

$$\frac{\dot{V}}{P_{av}} = \frac{1}{4}\frac{\delta}{\phi} \cdot \ln^2\left(2\frac{\phi}{\phi_{th}}\right) \tag{7}$$

All these considerations clearly show that the ablation process can be optimized. With the first derivation of (7) it is possible to calculate the threshold fluence:

$$\phi_{th} = \frac{2}{e^2}\phi_{opt} \tag{8}$$

with ϕ_{opt} the fluence of the optimal point of ablation. Out of equation (8) the maximum removal rate per average power (5) then reduces to:

$$\frac{\dot{V}_{max}}{P_{av}} = \frac{\delta}{\phi_{opt}} \tag{9}$$

With (8) and (9) it is possible to calculate the threshold fluence ϕ_{th} and energy penetration depth δ when the maximum ablation rate per average power and the corresponding optimal fluence are known.

For metals and pulses longer than 10 ps the threshold fluence begins to increase [8-10, 18]. But beside the threshold fluence also the penetration depth δ has an influence onto the maximum volume ablation rate. For pulse durations in the range from 10 ps to 50 ps the value of δ decreases with increasing pulse duration [8-10, 18]. Therefore the maximum removal rate in general drops significantly down when the pulse duration is raised. The situation changes for shorter pulses. From the literature [3] one expects that the threshold fluence will rest constant when the pulse duration becomes shorter than about 10 ps. If these pulses would lead to higher ablation rates this could only be caused by a higher penetration depth δ for shorter pulses.

Due to incubation effects the threshold fluence may strongly depend on the number of pulses applied, which is described for metals in [8, 9, 22, 25, 26]. Additionally it was found that also the energy penetration depth shows an incubation effect of the same kind. The maximum removal rate may therefore also strongly depend on the number of pulses applied; more details are given in [8-10, 22].

Modeling

All experimental data were fitted with the logarithmic ablation law (7) to get the threshold fluence ϕ_{th} and energy penetration depth δ. But in some measurements the ablation rates don't correspond to the expected rates (see Figure 1). The Peak and the sharp drop cannot be described with one threshold. In additional experiments with single pulses it can be shown that sometimes the ablation depth can be described with two or more logarithmic regimes as seen in Figure 2.

Therefore, a model with 2 thresholds was tested. For the ablation depth it reads:

$$z(\phi) = \begin{cases} 0, & \phi < \phi_1 \\ \delta_1 \cdot \ln^2\left(\dfrac{\phi}{\phi_{th,1}}\right), & \phi_1 \leq \phi < \phi_s \\ \delta_2 \cdot \ln^2\left(\dfrac{\phi}{\phi_{th,2}}\right), & \phi_s \leq \phi \end{cases} \quad (10)$$

with ϕ_s the fluence of the intersection of the two lines (black line in Figure 2). $\phi_{th,1}$ belongs to the red line and $\phi_{th,2}$ to the green line. Out of (10) the ablation rate per average Power changes:

$$\frac{\dot{V}}{P_{av}} = \frac{1}{\phi} \begin{cases} \dfrac{1}{4}\delta_1 \cdot \ln^2\left(\dfrac{2\phi}{\phi_{th,1}}\right), & \phi_1 \leq \phi < \phi_s \\ \dfrac{1}{4}\delta_1 \cdot \ln^2\left(\dfrac{2\phi}{\phi_{th,1}}\right) + \dfrac{1}{2}\delta_2 \cdot \ln\left(\dfrac{2\phi}{\phi_s}\right)\left(\ln\left(\dfrac{2\phi}{\phi_{th,2}} - \dfrac{1}{2}\ln\left(\dfrac{2\phi}{\phi_s}\right)\right)\right), & \phi_s \leq \phi \end{cases} \quad (11)$$

With (11) it is possible to fit the Peak, but not exactly the sharp drop. It fits better than the 1 threshold model.
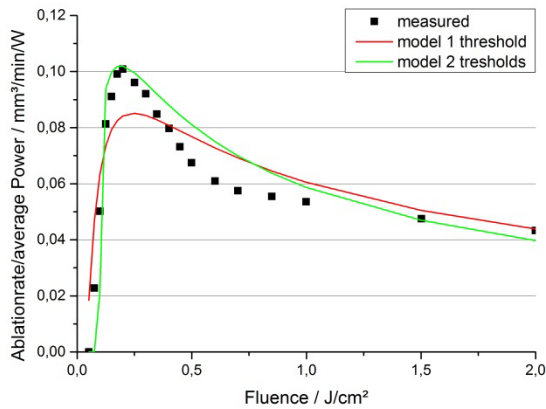

Figure 1: Ablation rate/average Power of hardened 1.3343
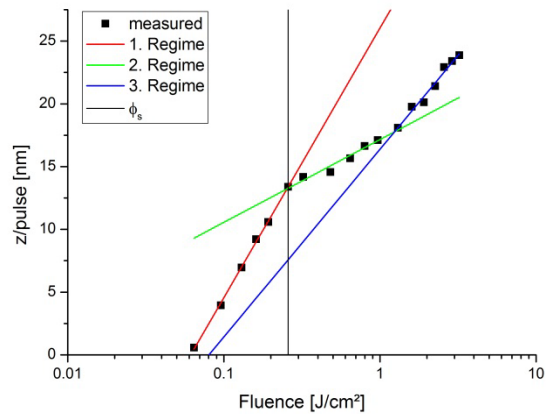

Figure 2: Ablation depth with 256 single pulses

But the 2 threshold model can only be applied if two thresholds are detected in experiments with single shots. Because it is very time-consuming to determine the single shot ablation depth for all experiments, it is not practicable. The following experiments will be done by ablating squares.

Because of the findings out of (7)-(9) the threshold fluence ϕ_{th} and energy penetration depth δ may be also determined from the maximum removal rate per average power. This maximum can be found by a parabolic fit to the data points around it. Out of this set of the maximal removal rate per average power and corresponding optimal fluence the threshold fluence ϕ_{th} and energy penetration depth δ can be calculated with (8) and (9).

Experimental Set-Up

The radiation of the used laser source was guided via a $\lambda/4$-plate (to generate a circular polarized beam) and folding mirrors through a beam expander into a galvo scanning head where it was focused by an f-theta objective onto the target. For the experiments three different laser systems were used:

The experiments for 10 ps and 50 ps were performed with a DUETTO[TM] (Time Bandwidth Products, Switzerland) ps-laser system working at a wavelength of 1064 nm with pulse duration of about 10 ps. By introducing corresponding etalon into the master oscillator the pulse duration was raised to 50 ps. The pulse duration was controlled with an autcorrelator measurement whenever the etalon was changed.

Helios 1062-5-50 (Coherent) is a ps-laser-system with pulse durations between 500 and 700ps. Here it works at 20 kHz repetition rate an 520ps pulse duration.

IPG YLMP-1 IR is an ns-laser-system. The experiments were performed with pulse duration of 4ns. As this laser was unpolarized it wasn't necessary to add a $\lambda/4$ plate

For all systems expect the IPG-laser beam quality factor M^2 was always better than 1.3. The IPG YLMP-1 IR has a beam quality factor M^2 of about 1.6. With all three laser systems hatched squares with a side length of 1 mm were machined into copper DHP and steel 1.4301, 1.3343(initial state and hardened) with a hatch distance of near the half of the spot radius. For better comparability, pulse repetition rate and focus radius should be kept approximately equal. The experiments with DUETTO (10, 50 ps) and the IPG-laser (4 ns) were done at 50 kHz and a focus radius of approximately 18 µm. The squares were machined with a hatch distance of 9 µm and a scan speed of

450 mm/s. Because of the suggested pulse duration Helios-system works only at 20 kHz with a spot radius of 15.3 µm. The squares were machined with a hatch distance of 8µm and a scan speed of 160 mm/s. The hatch angle was turned by 10° from slice to slice. This procedure was repeated 5 times to obtain a measurable depth of the squares.

For each pulse duration and material a series of squares with different average powers i.e. fluences were machined. On the one hand the depth of the ablated squares was measured with a KLA-Tencor Alpha-step IQ. On the other hand the absolute machining time was calculated from the marking speed, the side length, the hatch distance, the number of slices and the number of repeats. From this the removal rate could be calculated by dividing the ablated volume by the machining time and the average power. The threshold fluence and the energy penetration depth were then deduced via a least square fit of the model function (7) and from the maximum removal rate obtained by a parabolic fit to the measured data by using (8) and (9). The machined squares were additionally analyzed under an optical microscope to analyze the discoloring due to thermal effects.

Results

Ablation

Figure 3 and Figure 4 shows the measured removal rates and the corresponding least square fits with the model function (7) for copper and hardened 1.3343 as example for steel samples and the pulse duration of 50 ps. A quite good agreement between the experiment and the model can be observed. Similar results have also been achieved for all materials and longer pulse durations. For 10 ps a good agreement between experiment and model can achieved for copper and stainless steel 1.4301As described in the theory the sharp drop in the removal rate of steel 1.3343 could not be described with one threshold fluence. But because this drop located after the optimal point with maximum removal rate the 1 threshold model should provide useful results if this maximum is known. Therefore the maximum was also determined with a parabolic fit and out of this optimal point threshold fluence ϕ_{th} and energy penetration depth δ were determined with (8) and (9).
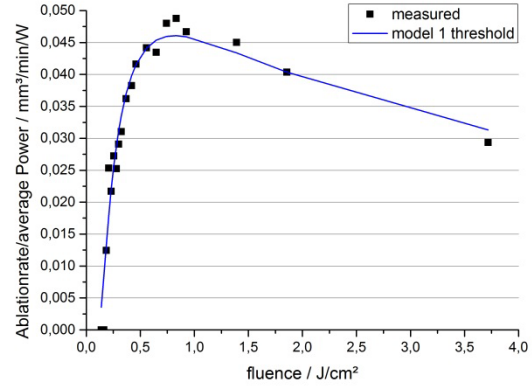

Figure 3: removal rates from the machined squares and the corresponding model function for copper and pulse duration of 50 ps
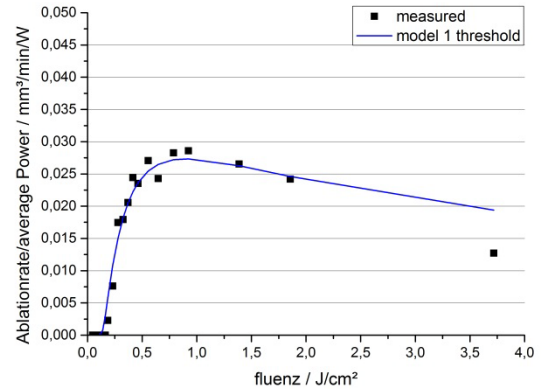

Figure 4: removal rates from the machined squares and the corresponding model function for hardened 1.3343 and pulse duration of 50 ps

The deduced threshold fluences, penetration depths and corresponding maximum removal rates are summarized for all pulse durations in Table 1 for copper, Table 2 for hardened 1.3343, Table 3 for initial 1.3343 and Table 4 for stainless steel 1.4301. For pulse durations longer than 50 ps the maximum removal rates first further drop until a minimum will be reached and then raise in the ns-regime. The minimum value is expected to be located between 100 ps and 1 ns and will depend on the material.

Table 1: Deduced threshold fluence, penetration depths and maximum removal rate for copper (1tm: 1 threshold model)

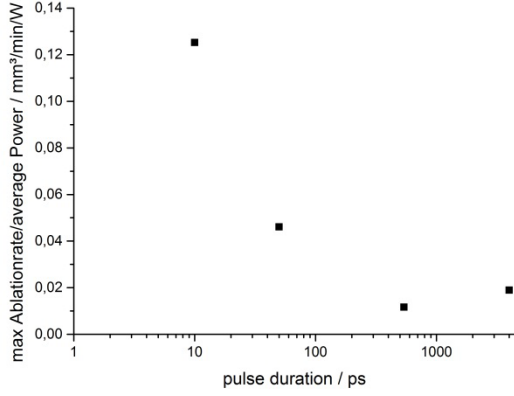|	$\Delta\tau$ / ps	#slices	ϕ_{th} / J/cm^2	δ / nm	$\Delta V_{max}/\Delta t$ / mm^3/min/W
1tm	10	5x18	0.29	22.5	0.13
1tm	50	5x 18	0.22	6.3	0.046
1tm	520	5x 18	0.9	6.5	0.012
1tm	4000	5x 18	0.51	5.92	0.019

Figure 5: Maximum removal rates as a function of the pulse duration for copper

This behavior of decreasing and increasing ablation depth per average power is exemplarily shown for copper in Figure 5.

For copper the threshold fluence ϕ_{th} for 520 ps is unexpected high. This experiment was difficult to analyze because the minimal ablation rate per average power seems to be around 500 ps. In the experiment only up to 4 µm depth could be reached with high fluences. Additionally the absorption rate for IR-light at 1064 nm is very low. The ablation was very inhomogeneous over the square and started at material defects like micro holes and cracks. Figure 9 illustrates this problem. On the left site some areas were ablated and others were not influenced by the laser beam. This behavior was observed only at 520 ps. For 4 ns ablation was homogeneous. This implies that heat accumulation has a significant influence to the threshold fluence of copper at pulse durations longer than 50 ps. The experiment should be repeated with more slices to be able to neglect the starting processes and get deeper squares for more accurate measurement. Therefore the experiment at 520 ps cannot be evaluated.

Table 2: Deduced threshold fluence, penetration depths and maximum removal rate for hardened 1.3343 (1tm: 1 threshold model, pf parabolic fit)

	$\Delta\tau$ / ps	#slices	ϕ_{th} / J/cm^2	δ / nm	$\Delta V_{max}/\Delta t$ / mm^3/min/W
1tm	10	5x18	0.07	3.48	0.085
pf	10	5x18	0.06	3.51	0.101
1tm	50	5x 18	0.24	4.12	0.027
pf	50	5x18	0.27	4.92	0.029
1tm	520	5x 18	0.7	2.67	0.006
1tm	4000	5x 18	0.75	6.3	0.014

Table 3: Deduced threshold fluence, penetration depths and maximum removal rate for initial 1.3343 (1tm: 1 threshold model, pf parabolic fit)

	$\Delta\tau$ / ps	#slices	ϕ_{th} / J/cm^2	δ / nm	$\Delta V_{max}/\Delta t$ / mm^3/min/W
1tm	10	5x18	0.06	3.76	0.096
pf	10	5x18	0.06	4.13	0.106
1tm	50	5x 18	0.22	3.82	0.027
pf	50	5x18	0.25	4.26	0.028
1tm	520	5x 18	0.61	2.38	0.006
1tm	4000	5x 18	0.74	5.97	0.013

Table 4: Deduced threshold fluence, penetration depths and maximum removal rate for 1.4301 (1tm: 1 threshold model, pf parabolic fit)

	$\Delta\tau$ / ps	#slices	ϕ_{th} / J/cm^2	δ / nm	$\Delta V_{max}/\Delta t$ / mm^3/min/W
1tm	10	5x18	0.05	3.55	0.117
pf	10	5x18	0.05	3.42	0.123
1tm	50	5x 18	0.13	2.29	0.028
pf	50	5x18	0.1	1.81	0.03
1tm	520	5x 18	0.56	2.5	0.007
1tm	4000	5x 18	0.69	5.98	0.014

For steel generally the course of maximal removal rate per average power is comparable to this of copper. Also the threshold fluence ϕ_{th} increases with increasing pulse duration. The absolute value depends on the material. For 1.4301 it is slightly lower than for 1.3343. This difference is quite pronounced at 50 ps where the threshold fluence ϕ_{th} for 1.4301 is about half of the value for 1.3343.

The energy penetration depth δ also depends on pulse duration and material composition. It shows a minimum which is located around 520 ps for 1.3343 and around 50 ps for 1.4301.

The difference between various steels is shown in Figure 6. Stainless steel 1.4301 has the highest removal rate per average power. The course is similar to the initial 1.3343 with slightly different threshold fluence ϕ_{th} (compare Table 2 and Table 4).

Hardened steel 1.3343 differs significantly from not hardened steel. As shown in Figure 1 the experimental data does not exactly follow the model from the logarithmic ablation law (7). After the maximum removal rate per average power a sharp drop is often observed. The threshold fluence ϕ_{th} is same for hardened and initial steel. The energy penetration depth δ is lower in the hardened state and the

maximum removal rate per average power is higher in initial state. Despite the sharp drop after the optimal point of ablation the values of threshold fluence ϕ_{th} and energy penetration depth δ deduced from the parabolic fit do only slightly differ from these obtained with the least square fit to the model (7).
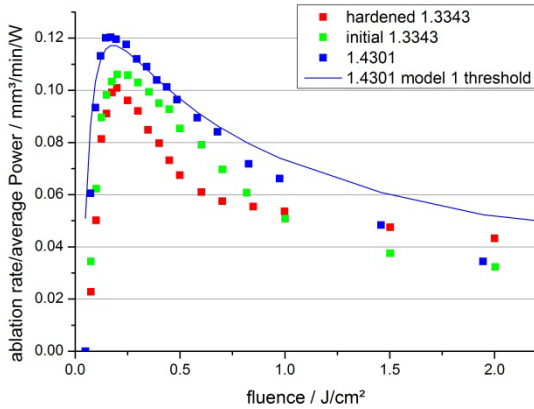

Figure 6: removal rates from the machined squares for steel and pulse duration 10 ps, corresponding model function for 1.4301

For increasing pulse duration this sharp drop does not occur anymore. Good agreement between experimental results and logarithmic ablation law could be achieved for pulse durations of 50 ps and longer for all steels. That implies that the effect, which is responsible for this sharp drop, decrease with increasing heat accumulation.

Surface quality

An overview of all ablated squares in steel 1.4301 is shown in Figure 7. The average power going with the pulse fluence is raised from left to right. The maximum power amounted about 3.7 W for 10 ps and 50 ps, 0.7 W for 520 ps and 2.2 W for 4 ns, respectively. For 10 ps and 50 ps the squares become black at higher powers due to crater formation which generally occurs at short pulse durations. This crater formation disappears for longer pulses but a thermal discoloration appears which is much stronger for 4 ns (see Figure 8).
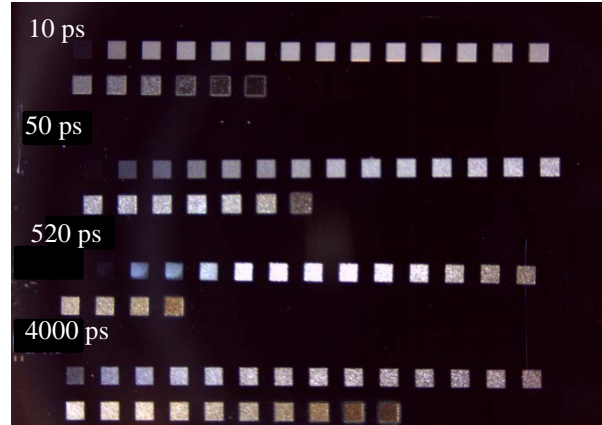

Figure 7: Overview of all machined squares in steel 1.4301. The fluence per pulse is raised from 1st line left to 2nd line right

Similar results without crater formation were obtained for copper. For the pulse duration of 520 ps at low fluences ablation was very inhomogeneous. Ablation starts at material defects like micro holes and cracks and widened with more slices until the whole square was ablated. For low fluences 90 slice were not enough to ablate the whole square. Figure 9 shows this behavior.
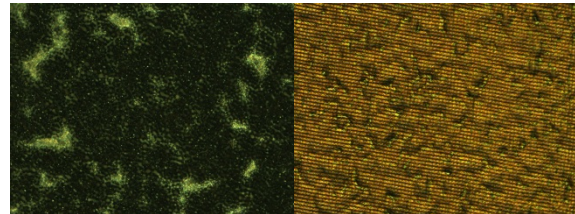

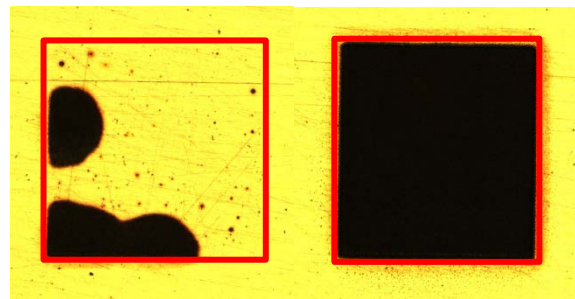Figure 8: Bottom of squares for 1.4301; left 10 ps, 1.9 J/cm²; right 4 ns, 3 J/cm²

Figure 9: Inhomogeneous ablation for copper at 520 ps pulse duration and low fluences, left 1.34 J/cm², right 1.5 J/cm², red square is the dimension of the ablated square

Conclusion

The range of pulse durations between 10 ps and 4 ns at the wavelength 1064 nm was investigated for copper and various steels concerning the removal rate. By

machining squares and measuring the removal rate the threshold fluence, the energy penetration depth and the maximum removal rate could be determined by a least square fit to a model for all investigated pulse durations. The trend of a decreasing removal rate with increasing pulse duration is confirmed up into the range of several 100 ps, but the trend is reversed when the pulse duration goes into the ns-regime. The behavior of the threshold fluence and the penetration depth indicates that heat conduction begins to dominate the energy transfer into the material when the pulse duration is raised from several 10 ps to several 100 ps. Further investigation have to be done for analyzing the surface quality of the ablated squares and get more information of melting in the ablation process.

An influence of material composition and crystalline structure is shown by analyzing various steels. Hardened material shows a sharp drop in removal rate per average power at short pulse durations, whereas this drop is less pronounced for the initial, not hardened material. Further investigations have to be done to check this influence of material composition and crystalline structure. Therefore different types of steel will be investigated in future to confirm this influence.

References

[1] B. N. Chichkov, C. Momma, S. Nolte, F. von Alvensleben and A. Tünnermann, „Femtosecond, picosecond and nanosecond laser ablation of solids", Appl. Phys. A 63, 109 (1996).

[2] Detlef Breitling, Andreas Ruf and Friedrich Dausinger, "Fundamental aspects in machining of metals with short and ulrashort laser pulses", Proc. SPIE 5339, 49-63 (2004)

[3] Friedrich Dausinger, Helmut Hügel and Vitali Konov, "Micro-machining with ultrashort laser pulses: From basic understanding to technical applications", Proc. SPIE Vol. 5147, 106-115 (2003)

[4] J. Meijer, K. Du, A. Gillner, D. Hoffmann, V. S. Kovalenko, T. Masuzawa, A. Ostendorf, R. Poprawe, W. Schulz, "Laser Machining by Short and Ultrashort Pulses – State of the Art", Annals of the CIRP, 51/2 (2002)

[5] S. Pierrot, J. Saby, B. Cocquelin and F. Salin, "High-Power all Fiber Picosecond Sources from IR to UV", Proc. of SPIE Vol. 7914, paper 79140Q (2011)

[6] S. Kanzelmeyer, H. Sayinc, T. Theeg, M. Frede, J. Neumann and D. Kracht, "All-fiber based

amplification of 40 ps pulses from a gain-switched laser diode", Proc. of SPIE Vol. 7914, paper 191411 (2011)

[7] P Deladurantaye, A. Cournoyer, M. Drolet, L. Desbiens, D. Lemieux, M. Briand and Y. Taillon, "Material micomachining using bursts of high repetition rate picoseconds pulses from a fiber laser source", Proc. of SPIE Vol. 7914, paper 791404 (2011)

[8] M. Schmid, B. Neuenschwander, V. Romano, B. Jaeggi and U. Hunziker, "Processing of metals with ps-laser pulses in the range between 10ps and 100ps", Proc. of SPIE Vol. 7920, paper 792009 (2011)

[9] B. Jaeggi, B. Neuenschwander, M. Schmid, M. Muralt, J. Zuercher and U. Hunziker, "Influence of the Pulse Duration in the ps-Regime on the Ablation Efficiency of Metals", Physics Procedia 12, 164-171 (2011)

[10] B. Neuenschwander, B. Jaeggi, M. Schmid, U. Hunziker, B. Luescher, C. Nocera, "Processing of industrially relevant non metals with laser pulses in the range between 10 ps and 50 ps", ICALEO 2011, Paper M103 (2011)

[11] B. Sallé, O. Gobert, P. Meynadier, G. Petite and A. Semerok, "Femtosecond and picosecond laser microablation: ablation efficiency and laser microplasma expansion", Appl. Phys. A 69[Suppl.], 382 – 383 (1999)

[12] R. Le Harzig, D. Breitling, M. Weikert, S. Sommer, C. Föhl, S. Valette, C. Donnet, E. AUdouard and F. Dausinger, "Pulse width and energy influence on laser micromachining of metals in a range of 100 fs to 5 ps", Appl. Surf. Science 249, 322-331 (2005)

[13] J. Lopez, A. Lidolff, M. Delaigue, C. Hönninger, S. Ricaud and E. Mottay, "Ultrafast Laser with high Energy and high average power for Industrial Micromachining: Comparision ps-fs", ICALEO 2011, Paper 401 (2011)

[14] P. Russbueldt, T. Mans, J. Weitenberg, H.-D. Hoffmann, R. Poprawe, "Compact diode-pumped 1.1 kW Yb:YAG Innoslab femtosecond amplifier," Opt. Lett. 35, 4169-4171 (2010)

[15] P. Russbueldt, T. Mans, H-D. Hoffmann, R. Poprawe, "1100 W Yb:YAG femtosecond Innoslab amplifier", Proc. of SPIE, 7912 (2011)

[16] C. Momma, B.N. Chichkov, S. Nolte, F. van Alvensleben, A. Tünnermann, H. Welling and B.

Wellegehausen, "Short-pulse laser ablation of solid targets", Opt. Comm. 129, 134-142 (1996)

[17] C. Momma, S. Nolte, B.N. Chichkov, F. van Alvensleben and A. Tünnermann, "Precise laser ablation with ultrashort pulses", Appl. Surf. Science 109/110, 15-19 (1997)

[18] S. Nolte, C. Momma, H. Jacobs, A. Tünnermann, B.N. Chichkov, B. Wellegehausen and H. Welling, "Ablation of metals by ultrashort laser pulses", J. Opt. Soc. Am. B, Vol. 14, No. 10 (1997)

[19] S.I. Anisimov and B. Rethfeld, "On the theory of ultrashort laser pulse interaction with a metal", Proc. SPIE 3093, 192-203 (1997)

[20] B.H. Christensen, K. Vestentofrt and P. Balling, "Short-pulse ablation rates and the two-temperature model", Appl. Surf. Science 253, 6347-6352 (2007)

[21] P. Mannion, J. Magee. E. Coyne and G.M. O'Conner, "Ablation Thresholds in ultrafast laser micro-machining of common metals in air", Proc. of SPIE vol. 4876, 470-478 (2002)

[22] B. Neuenschwander et al., "Optimization of the volume ablation rate for metals at different laser pulse-durations from ps to fs", Proc. of SPIE vol. 8243, 824307-1 (2012)

[23] B. Neuenschwander, G. Bucher, C. Nussbaum, B. Joss, M. Muralt, U. Hunziker et al., "Processing of dielectric materials and metals with ps-laserpulses: results, strategies limitations and needs", Proceedings of SPIE vol. 7584, (2010)

[24] G. Raciukaitis, M. Brikas, P. Gecys, B. Voisiat, M. Gedvilas, "Use of High Repetition Rate and High Power Lasers in Microfabrication: How to keep Efficiency High?", JLMN Journal of Laser Micro/Nanoengineering, Vol. 4 (3), 186-191 (2009)

[25] Y. Jee, M.F. Becker and R.M. Walser, "Laser-induced damage on single-crystal metal surfaces", J. Opt. Soc. Am. B5, (1988)

[26] P.T. Mannion, J. Magee, E. Coyne, G.M. O'Connor and T.J. Glynn, "The effect of damage accumulation behavior on ablation thresholds and damage morphology in ultrafast laser micro-machining of common metals in air", Appl. Surface Science 233, 275 – 287 (2004)